Supporting Information

Enhancing red upconversion luminescence of hybrid porous microtubes via in situ O-substituted reaction through heat treatment

Dangli Gao,[*ac] Jie Gao,[a] Dan Zhao,[a] Qing Pang,[a] Guoqing Xiao,[b] Liangliang Wang[c] and Kaiwei Ma[a]

a. College of Science, Xi'an University of Architecture and Technology, Xi'an 710055, China

b. College of Materials and Mineral Resources, Xi'an University of Architecture and Technology, Xi'an 710055, China

c. Shaanxi Key Laboratory of Nano Materials and Technology, Xi'an University of Architecture and Technology, Xi'an 710055, China

*Corresponding Author

Email: gaodangli@163.com

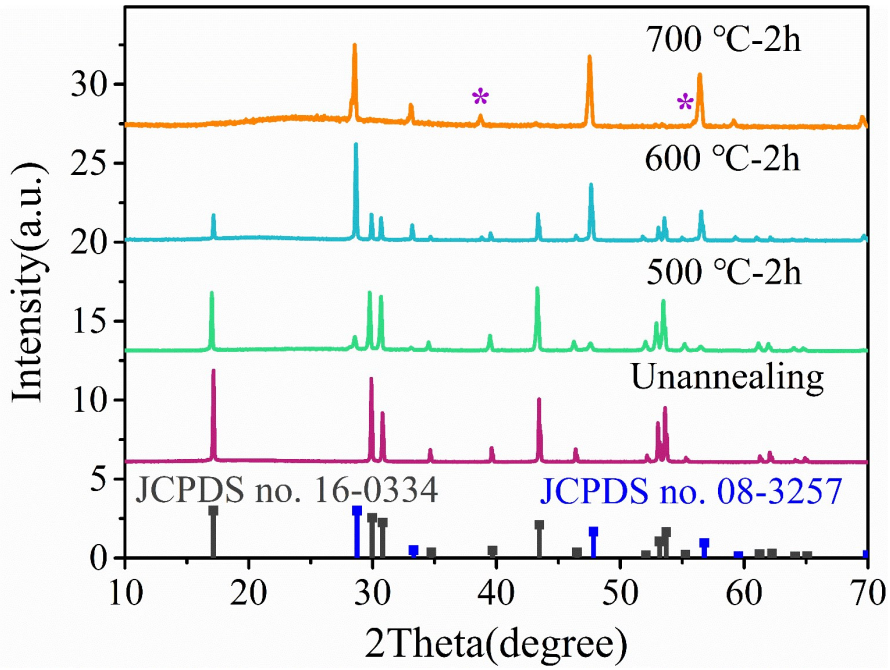

Fig. S1 XRD patterns of $NaYF_4$:Yb/Er (20/1 %) microtubes before and after annealing. The annealing temperatures are marked in figure. Note that the bottom of the panel is standard data for hexagonal $NaYF_4$ (dark gray, JCPDS no. 16-0334) and cubic YOF (blue, JCPDS no. 08-3257). The purple stars are the peaks from NaF crystals.

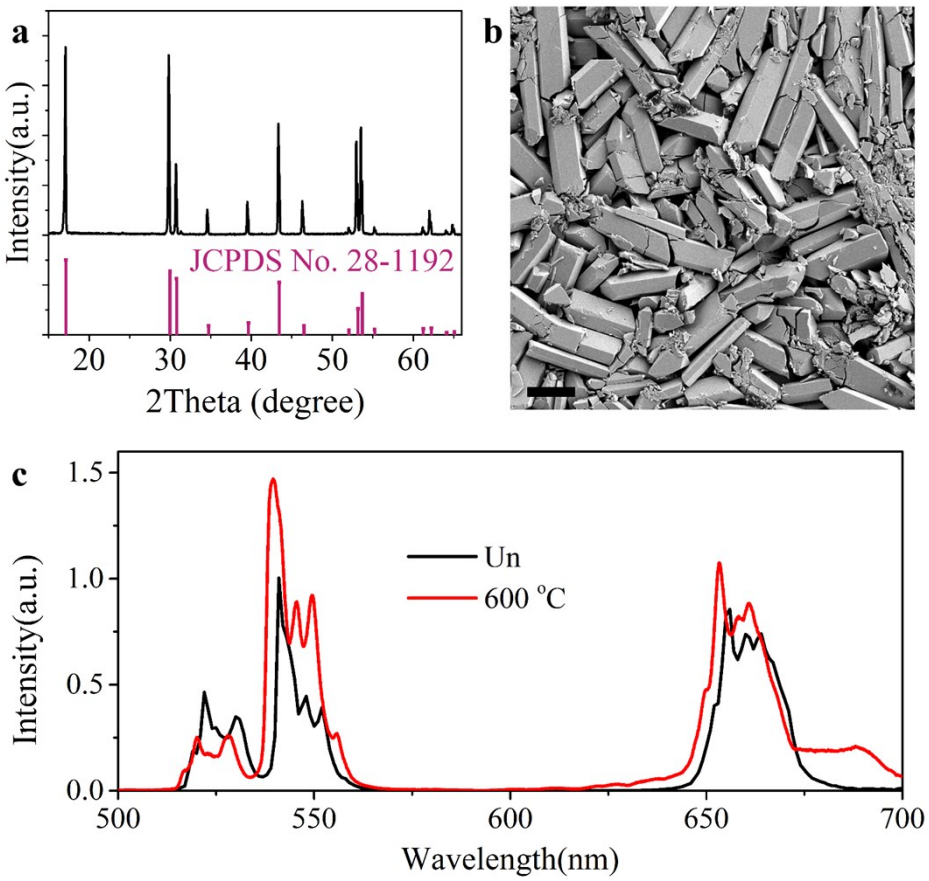

Fig. S2 Typical XRD, SEM images and the UC emission spectra of $NaYF_4$: Yb/Er (20/1 %) microtubes after annealing at 600 ℃ in N_2 atmosphere.

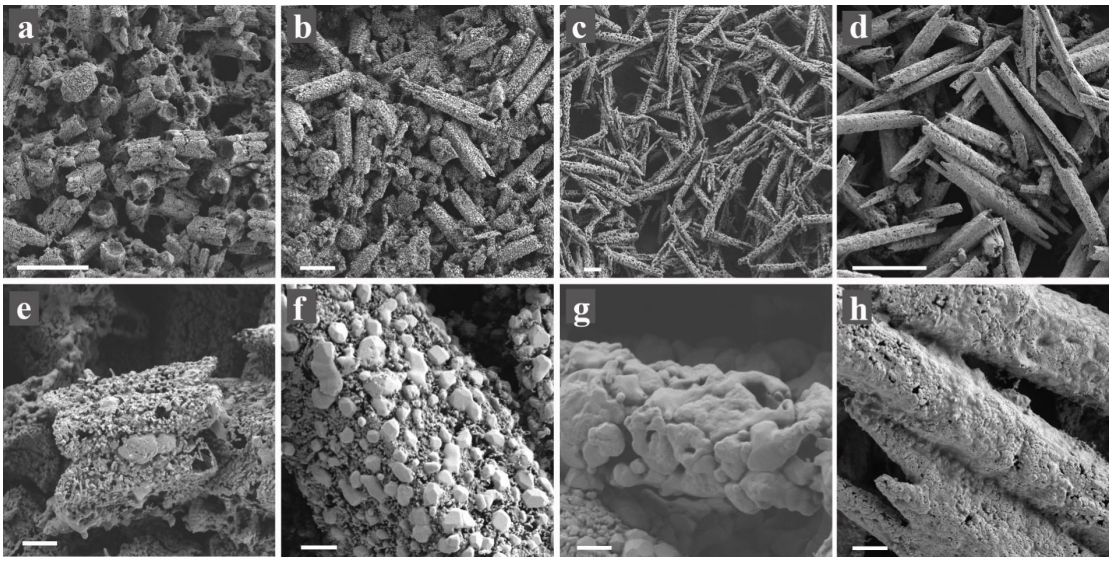

Fig. S3 Typical SEM images of $NaYF_4$:Yb/Er microtubes doped with transition elements such as Mn^{2+} or Cr^{3+} after annealing at 700 ℃. (a,e) $NaYF_4$:Yb/Mn/Er (20/20/1 %); (b,f) $NaYF_4$:Yb/Mn/Er (20/40/1 %); (c,g) $NaYF_4$:Yb/Cr/Er (20/20/1%); (d,h) $NaYF_4$:Yb/Cr/Er (20/40/1 %). Scale bar: (a-d) 10 μm; (e-h) 1 μm.

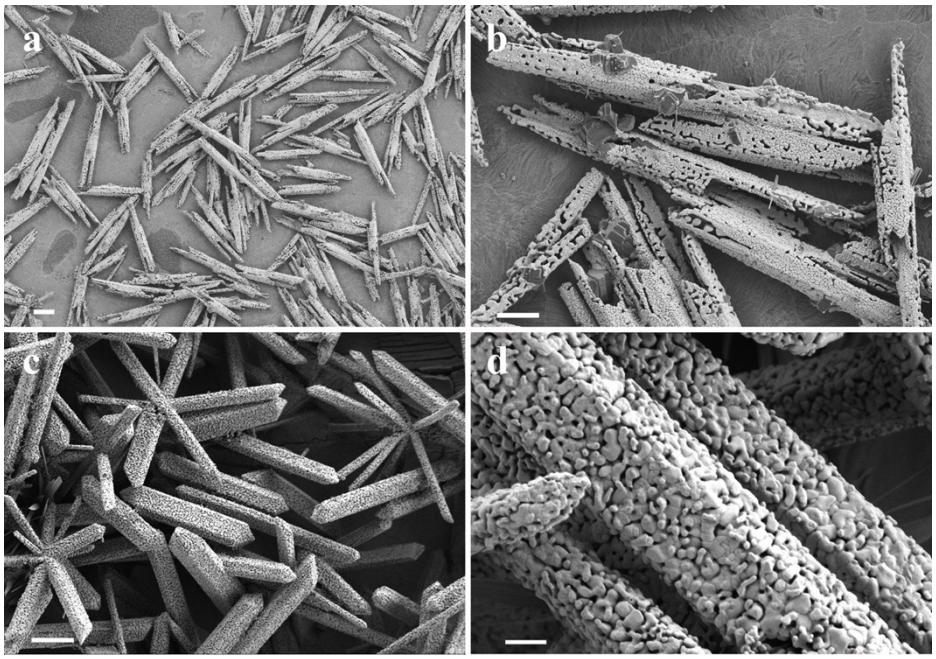

Fig. S4 Typical SEM images of $NaYF_4$:Yb/Er (40/1 %) microtubes (a,b) and microrods (c,d) after annealing at 750 ℃. Scale bar: (a) 10 μm, (b,c) 5 μm and (d) 1 μm.

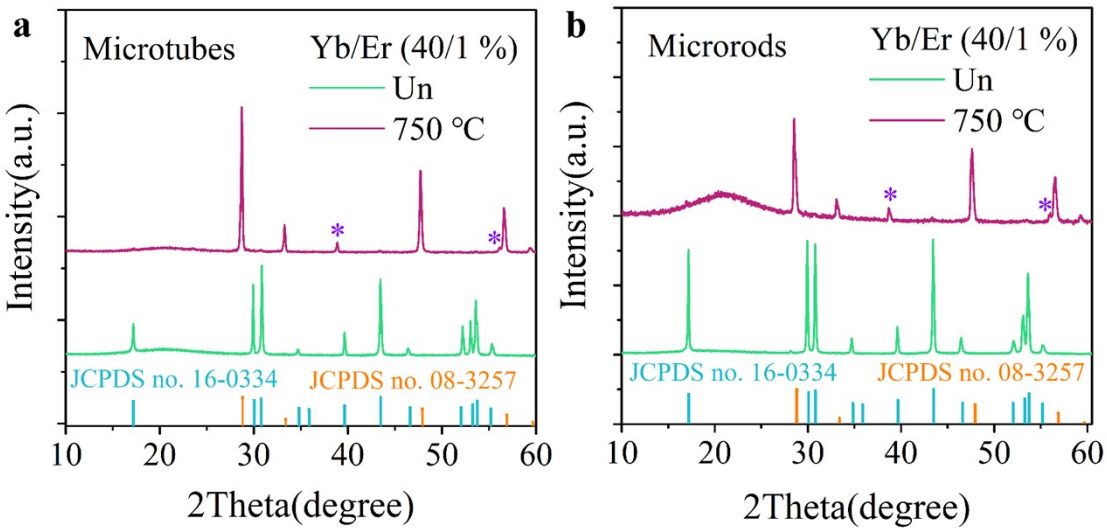

Fig. S5 XRD patterns of $NaYF_4$:Yb/Er (40/1 %) microtubes (a) and microrods (b) before and after annealing at 750 ℃ for 2 hours, respectively. The standard data for hexagonal $NaYF_4$ (JCPDS no. 16-0334) and cubic YOF (JCPDS no. 08-3257) are marked in the bottoms. The purple stars are the peaks from NaF crystals.

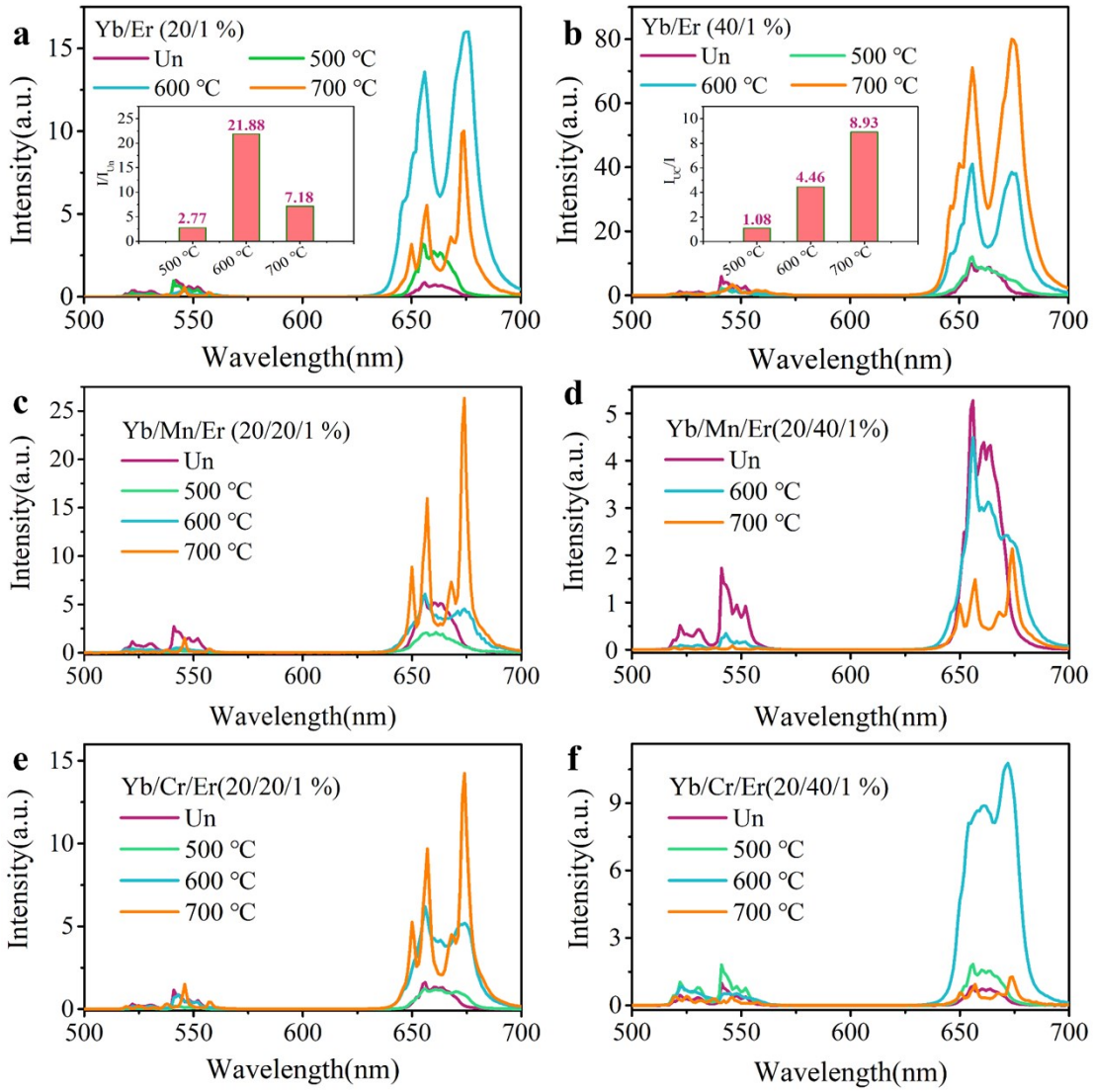

Fig. S6 Emission spectra of $NaYF_4$:Yb/Er microtubes with or without Mn^{2+} or Cr^{3+} doping. Noted that the insets of (a) and (b) are the integrated luminescence intensities ratios of as-prepared samples after annealing to the corresponding maternal $NaYF_4$:Yb/Er(20/1 %) and $NaYF_4$:Yb/Er(40/1 %) microtubes, respectively. All the samples were excited with a 980 nm laser operating at 200 mW/cm^2. Therein, (a) $NaYF_4$:Yb/Er(20/1 %), (b) $NaYF_4$:Yb/Er (40/1 %), (c) $NaYF_4$:Yb/Mn/Er (20/20/1 %), (d) $NaYF_4$:Yb/Mn/Er (20/40/1 %), (e) $NaYF_4$:Yb/Cr/Er (20/20/1 %) and (f) $NaYF_4$:Yb/Cr/Er (20/40/1 %).

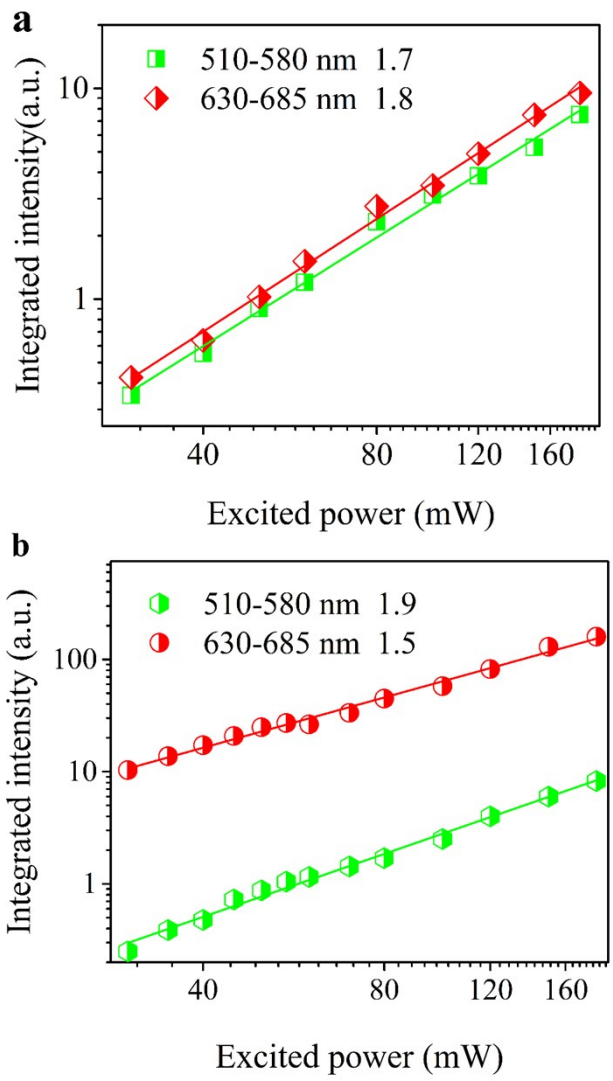

Fig. S7 Ln–ln variation curves of green and red UC luminescence intensity upon laser power densities for (a) $NaYF_4$:Yb^{3+}/Er^{3+}(20/1 %) and (b) $NaYF_4$:Yb^{3+}/Er^{3+}(20/1 %)@YOF:Yb^{3+}/Er^{3+}(20/1 %) (600 °C, Air) samples under 980 nm excitation.

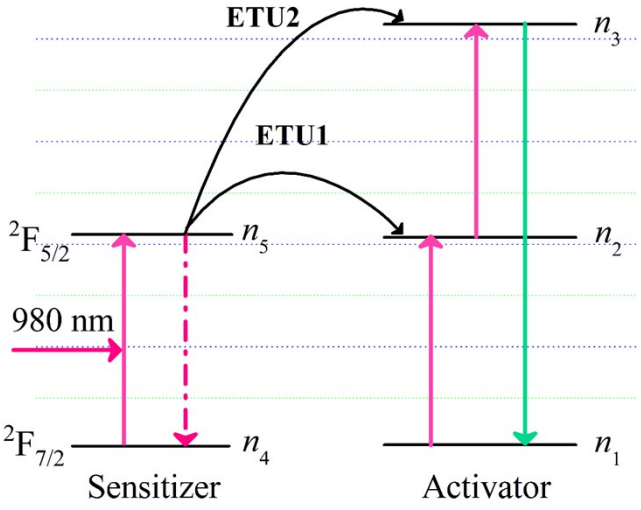

Fig. S8 A standard two-photon UC mechanism in our UC systems. Energy transfer UC (ETU), from the sensitizer to the activator, is considered as the primary UC mechanism.

In this typical two-photon UC process as shown in Fig. S8, the activator ion at the ground state (state 1) is first excited to state 2 through an ETU process (ETU1), and further excited to state 3 through a second ETU process (ETU2). The UC luminescence is generated from the transition 3→1. The time-dependent populations of different energy states can be described by the following rate equations:

$$\text{State 1: } \frac{dn_1}{dt} = -W_1 n_5 n_1 + \frac{n_2}{\tau_2} + \frac{n_3}{\tau_3} \tag{1}$$

$$\text{State 2: } \frac{dn_2}{dt} = W_1 n_5 n_1 - W_2 n_5 n_2 - \frac{n_2}{\tau_2} \tag{2}$$

$$\text{State 3: } \frac{dn_3}{dt} = W_2 n_5 n_2 - \frac{n_3}{\tau_3} \tag{3}$$

$$\text{State 4: } \frac{dn_4}{dt} = -\frac{\sigma\rho(t)}{h\nu} n_4 + \frac{n_5}{\tau_5} + W_1 n_5 n_1 + W_2 n_5 n_2 \tag{4}$$

$$\text{State 5: } \frac{dn_5}{dt} = \frac{\sigma\rho(t)}{h\nu} n_4 - \frac{n_5}{\tau_5} - W_1 n_5 n_1 - W_2 n_5 n_2 \tag{5}$$

$$n_1 + n_2 + n_3 = n_A \tag{6}$$

$$n_4 + n_5 = n_S \tag{7}$$

Where $\rho(t)$ is time-dependent excitation power density, W_i represents the rate constants of the energy transfer processes, τ_i is the lifetime of the excited energy levels, and σ is absorption cross-section of the sensitizer ions.

Based on rate equations, when the sensitizer's excited-state lifetime τ_5 is significantly smaller than τ_3, the decay behavior of UCL can be well represented by its natural decay characterized by τ_3. With increasing τ_5, the induced UCL decay starts to gradually deviate from its natural decay. When $\frac{\tau_5}{\tau_3}$ reaches 10, the UCL decay profile can approach an exponential decay curve characterized by a time constant of $\frac{\tau_5}{2}$ (or $5\tau_3$). In our present case, the luminescence lifetime is dominated due to $\frac{\tau_5}{\tau_3} \geq 10$, while τ_5 mainly depends on W_i. Hence, shortening the decay time after annealing suggests the improvement of energy transfer efficiency. The reduced rise time of time evolution profile of luminescence supports this conclusion.

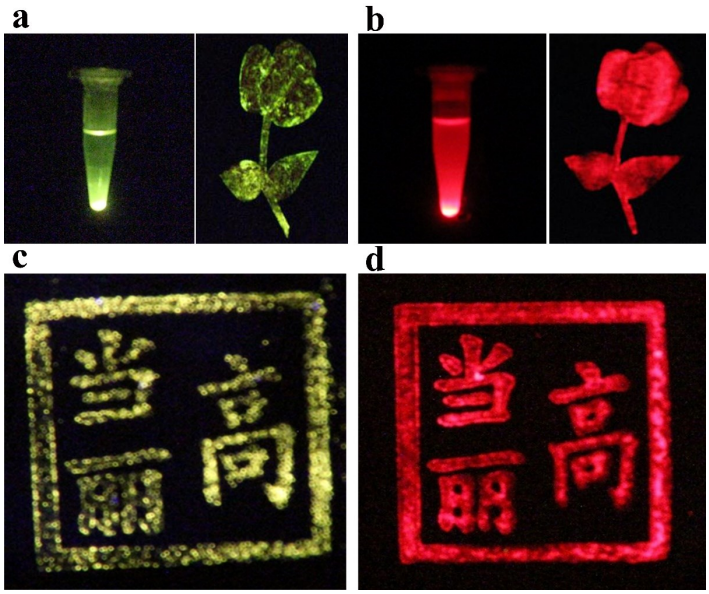

Fig. S9 Luminescence photos under 980 nm excitation with 400 mw/cm^2 power density. Noted that (a,b) $NaYF_4$:Yb/Er (40/1 %) microtubes before and after annealing at 600 ℃ as green and red inks, respectively; (c,d) $NaYF_4$:Yb/Er (60/1 %) microtubes before and after annealing at 600 ℃ as green and red inks, respectively.

Table 1 Decay times for green and red UC luminescence in $NaYF_4$:Yb/Er(20/1%) microtubes under 980 nm excitation.

Sample	$\tau_{546\,nm}$ [μs]	$\tau_{656\,nm}$ [μs]
Un	456 ± 5	317 ± 5
500 ℃	110 ± 5	134 ± 5
600 ℃	160 ± 5	183 ± 5
700 ℃	278 ± 5	280 ± 5